

Adaptive Simulation of Electrical Discharges

Bernd Bickel Martin Wicke Markus Gross

Computer Graphics Laboratory, ETH Zurich
Email: {bickel, wicke, grossm}@inf.ethz.ch

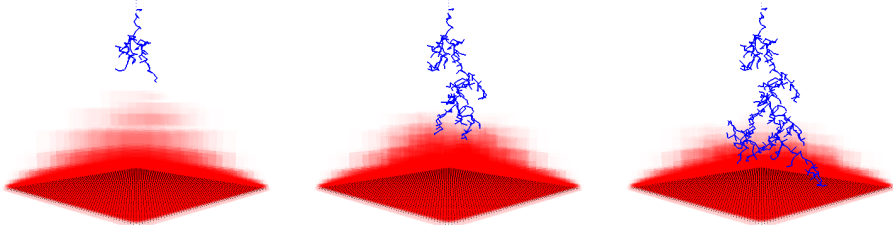


Figure 1: *Simulation of a cloud-to-ground lightning. The breakdown pattern is computed iteratively using the dielectric breakdown model on an adaptively sampled grid.*

Abstract

We present an adaptive animation method for electrical discharges. Electric discharges can be simulated using the dielectric breakdown model. Regular discretization of the governing Laplace equation leads to huge equation systems, and the computational cost of solving the equations quickly becomes prohibitive at high resolutions, especially for simulations in 3D. In contrast, our method discretizes the Laplace equation on an adaptive octree, reducing the size of the problem significantly, and making simulations of high resolution 3D datasets and even 3D animations feasible.

In order to enhance realism for lightning animations, we propose a particle simulation that animates the residual positive charge. Thus, interaction of electrical discharges with their surroundings can be simulated.

1 Introduction

Electrical discharges result from high charge differences between objects. In nature, we can observe very appealing visual effects due to electrical discharges, such as intracloud discharges or cloud-to-ground lightnings.

From the earliest days of cinema, electric discharges have played an important role in movies. Consequently, there has been some research in the

field of computer graphics related to animation of electrical discharges. Most of this work is limited to still images and unsuited for animation purposes.

Recently, Kim and Lin [1] proposed a physically-based approach to lightning simulation. While their approach can produce animations, their regular space discretization generates huge equation systems that have to be solved many times. For high-resolution data sets, especially 3D datasets, the computation time quickly becomes prohibitive.

Our contributions can be summarized as follows:

- We propose an adaptive discretization that dramatically reduces the size of the resulting equation systems. We can thus compute high-resolution 3D animations, while maintaining a high-quality physical simulation.
- In order to enable interaction between the electrical discharge and its environment, we simulate the residual positive charge (RPC) left behind by individual lightning strokes. Using a particle simulation, residual positive charge is influenced by its surrounding media and vice versa.

The remainder of this paper is organized as follows: We will first discuss related work in Section 2. Section 3 presents the dielectric breakdown model (DBM). In Section 4, our adaptive space discretization is described. Section 5 introduces the RPC simulation and the rendering is described Section 6. Finally, we show results in Section 7 and conclude.

2 Related Work

One of the first quantitative investigations of the geometry of lightning strokes [2] was done by Hill [3]. LeVine and Gilson [4] analyzed photographs and investigated branching and segment length.

As the physics of an electric breakdown is complicated and computationally expensive to simulate, Reed and Wyvill [5] propose a method that exploits the geometrical properties and uses a probability function to control the branching. They concatenate linear segments with direction chosen from a normal distribution with mean 16 degrees and variance of 0.1. Their model was extended by Glassner [2] who extracts parameters for branch length, branch frequency, and branching angle from a data set of 40 digitized strokes. In a second pass, they enhance the structure by adding "tortuosity". Kruszewski [6] uses a procedural model based on random binary trees for constructing the branching pattern. All of these models do not take the electric field and charge distribution into consideration.

In computer graphics, the dielectric breakdown model (DBM) was first used by Sosorbaram et al. [7] to generate branches of electrical discharges, although the potential field was not computed based on the Laplace equation. Kim and Lin [1] extend the method to simulate sustained electrical discharges and solve the full Laplace equation.

The DBM has also been used in the field of geophysical research (meteorology and atmospheric dynamics) [8].

Recently, Kim et al. [9] proposed a particle-based method for fast fractal growth, but their approach does not solve the Laplace equation.

A good overview of solution techniques for the Laplace and Poisson equation on regular domains can be found in [10], on irregular domains see e.g. [11, 12, 13]. Furthermore, multigrid methods [14] and adaptive mesh refinement techniques [15, 12] allow efficient resolution and lower the computational effort.

The visualization of lighting is challenging mainly because of atmospheric scattering that creates the typical glow of lightning channels. Dobashi et al. [16] present a method that precomputes atmospheric effects, and stores the intensity of scattered light in a lookup table. Other methods use either a simple volume rendering approach [7], or are adding a color contribution from lightning using a shading method designed for raytracing [5]. Simi-

lar to Kim and Lin [1], we use the atmospheric point spread function (APSF) introduced by Narasimhan et al. [17] which describes the glow of a point light source under specific weather conditions.

3 Physically-based Simulation of Electrical Discharges

The most frequent natural discharge phenomena during a thunderstorm is negative cloud-to-ground lightning, where there is a high concentration of negative charge at the bottom of the cloud. If the charge difference between cloud and ground passes a certain threshold, an electrical breakdown occurs. Stepwise, small lightning channels evolve from the cloud toward the ground, forming a forked pattern. As soon as one of these channels reaches the ground, a discharge (lightning stroke) takes place. Typically, lightning consists of several consecutive strokes, where the first is called *stepped leader* and the successive strokes *dart leaders*. As Kim and Lin [1] has shown, this can be simulated using a modified version of the dielectric breakdown model (DBM) developed by Niemeyer et al. [18].

In the remaining section, we will describe the original DBM, which is only capable of simulating stepped leaders, and its modification by Kim and Lin, that also takes dart leaders into account.

3.1 Dielectric Breakdown Model

The basic assumption of the DBM is that the dielectric breakdown of insulators depends on the local electric field. The emerging discharge channels show a strong tendency to branch into complicated

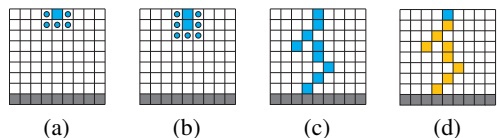


Figure 2: Schematic illustration of the DBM. From left to right: (a) Initial boundary conditions for a downward negative lightning (blue $\phi = 0$, gray $\phi = 1$). Blue points indicate the set N of possible breakdown locations. (b) shows the breakdown after one iteration, (c) after it has reached the ground. (d) shows the initial configuration for simulating a dart leader. Residual positive charge is marked orange.

stochastic patterns, with a fractal dimension of approximately 1.7 [18].

These patterns can be simulated on a discrete lattice, where ϕ_i captures the electric potential of node n_i . The breakdown is modeled as an iterative stochastic process, where the probability of a breakdown is related to the electric potential field, which is computed by solving the Laplace equation. Clouds, ground, and the already computed breakdown are treated as boundary conditions (see colored cells in Figure 2). At the beginning of the simulation, a subset N of nodes is selected, which mark possible locations where a breakdown could occur (indicated as blue dots in Figure 2 (a)). In each step, one node $n_s \in N$ is selected as location of the next breakdown, and N is updated by removing the selected node n_s and adding all adjacent nodes of n_s that are not yet part of the lightning (Figure 2 (b)). During the simulation, all nodes that are part of the lightning stroke are considered as equipotential ($\phi_{lightning} = 0$), and n_s is added to the set of boundary cells.

The probability p that a node of N is selected is given by the equation

$$p(n_i) = \begin{cases} \frac{(\phi_i)^\eta}{\sum_{k \in N} (\phi_k)^\eta} & \text{if } n_i \in N \\ 0 & \text{otherwise.} \end{cases} \quad (1)$$

The user-defined parameter η controls the relationship between potential field and probability. A low value leads to dense branching, and with increasing η the branching density decreases. For a detailed discussion of this parameter see [19, 20]. To draw a node, we assign each node an interval in $[0, 1]$ according to equation (1) and use a uniform random number generator. This yields the propagation of the lightning and at the same changes the boundary condition, therefore the electrical field ϕ has to be recomputed by solving the Laplace equation $\nabla^2 \phi = 0$ in each step. The simulation stops as soon as the lightning reaches the ground or any other cell that is marked as a boundary with $\phi > 0$.

As already mentioned, initial charge distribution and the already computed breakdown pattern are treated as boundary conditions. Depending on the lightning type we want to simulate, the initial charge distribution has to be set appropriately. In case of negative cloud-to-ground lightning, as illustrated in Figure 2 (a), cells with potential $\phi = 0$ are placed at the position of the cloud. All adjacent cells to the cloud are handled as locations of

possible initial breakdowns and are therefore added to N . Cells at the ground are set to $\phi = 1$. Note that due to the flexibility of arbitrarily setting the boundary conditions, a very wide range of lightning types and electric breakdowns can be simulated, such as cloud-to-ground, intracloud, cloud-to-cloud, or ground-to-cloud lightning [7].

Once the initial stepped leader has shaped, we adopt the method by Kim and Lin [1] that hypothesizes that residual positive charge along the path of the stepped leader causes dart leaders to follow approximately the path of the initial leader. The Poisson equation $\nabla^2 \phi = -4\pi\rho$ allows the computation of the potential field ϕ under consideration of this effect [1, 21]. Residual positive charge is quantified by ρ . The bigger ρ is for a node, the stronger it will attract a new dart leader. Poisson equation and its homogeneous form, the Laplace equation, are identical except for the right hand side, so both can be handled by the same routine if the residual positive charge is initialized appropriately. Figure 2 shows a schematic illustration of a downward negative lightning simulation.

4 Adaptive Discretization

Observing that the behavior of the potential field ϕ is smooth and high spatial resolution is only needed close to the evolving lightning for propagation computation, we propose an adaptive discretization of space.

Two simple rules govern the generation of an adaptive grid. Cells adjacent to fixed potentials, such as the breakdown pattern, must have the smallest possible size, and the edge length of neighboring cells differ at most by a factor of two. Figure 3 shows an example of the adaptive discretization in 2D.

Assigning the smallest possible size to cells adjacent to fixed potentials guarantees that we can simulate the growth of the stepwise breakdown as exact as possible. The set N of possible breakdown locations is always in cells of the highest resolution. Limiting the edge length differences by a factor of two results in smooth changes of the local sampling density.

We implemented the data structure using an octree and subdivide the cells according to the rules mentioned above. The initial charge distribution is inserted at the finest level.

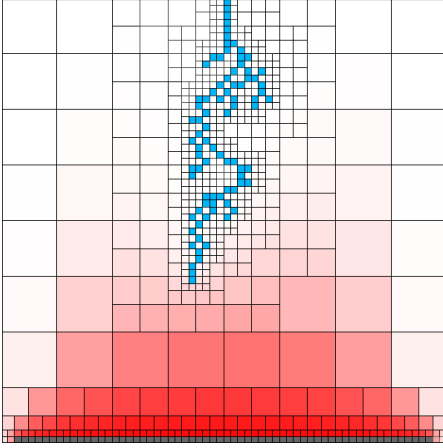


Figure 3: *Adaptive Discretization in 2D.* The discharge pattern is marked blue, positive charges at the ground gray, and the potential field ϕ red. Note that the size of adjacent cells differs at most by a factor of two.

Guaranteeing on the one hand highest resolution close to the evolving lightning while on the other hand saving memory and CPU resources due to a coarser representation in the remaining computational domain enables us to animate thunderstorms within a reasonable amount of time.

4.1 Interpolation

For solving the Laplace or Poisson equation, the second derivative is approximated using a seven-point finite differences scheme in 3D [22]. On a uniform grid, it uses the values of the center of the cell and its direct neighbors, which all have the same distance from the center value, as shown in Figure 4 (a). In our data structure adjacent cells can be smaller or larger, thus we interpolate values at the locations needed for the finite difference scheme.

A straightforward solution would be to interpolate values on each side of the cell that all have the same distance to the center. However, in case of smaller neighbor cells, computing the interpolation can involve a large number of smaller cells in the neighborhood, as illustrated in Figure 4 (b). Using this interpolation in combination with finite differences for setting up the Laplace or Poisson equation can result in a non-sparse system. Therefore we use a seven-point finite difference scheme that takes different distances to adjacent values into ac-

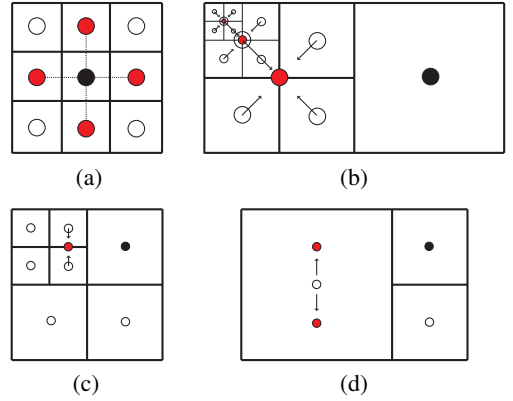


Figure 4: *Setting up the finite-difference approximation for the cell with the bold black dot.* (a): Finite differences using equal distances to all neighbors. (b): Computing the average at the center position of a fictive equally sized adjacent cell could involve a large number of cells. (c): In case of smaller adjacent cells, the value at the position of the red dot is approximated. (d): In case of a larger adjacent cells, the value is shifted.

count [22], which gives us more freedom for choosing the interpolation location:

$$\nabla^2 \phi = \frac{\partial^2 \phi(x,y,z)}{\partial x^2} + \frac{\partial^2 \phi(x,y,z)}{\partial y^2} + \frac{\partial^2 \phi(x,y,z)}{\partial z^2}. \quad (2)$$

$$\frac{\partial^2 \phi(x,y,z)}{\partial x^2} \approx \frac{2\phi(x+h_r,y,z)}{(h_l+h_r)h_r} - \frac{2\phi(x,y,z)}{h_l h_r} + \frac{2\phi(x-h_l,y,z)}{(h_l+h_r)h_l},$$

where h_l and h_r are the distances to the left respectively right neighboring cell centers; $\partial^2 \phi(x,y,z)/\partial y^2$ and $\partial^2 \phi(x,y,z)/\partial z^2$ are defined similarly.

This scheme requires that for each cell there is exactly one neighboring point on each side, lying on the axis which is going through the center of the cell.

In our octree-based discretization, in case of smaller neighboring cells, we take the average of the adjacent cells, as shown in Figure 4 (c). In case of a larger neighboring cell, their centered value is shifted slightly (Figure 4 (d)). For each cell, there is now exactly one neighboring point on each side, going through the axis of the center of the cell. By using only adjacent cells for the interpolation, we can guarantee that the number of involved cells is limited, because the size of adjacent cells differs at most by a factor of two.

Substituting the finite-difference approximation

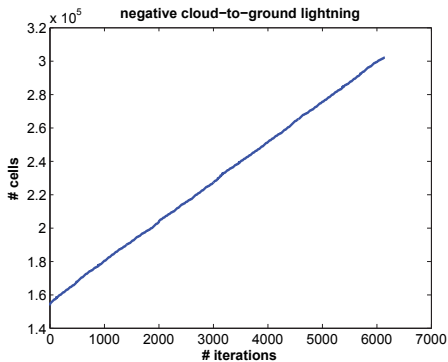


Figure 5: Adaptive sampling: Number of cells during the simulation of a downward negative lightning (stepped leader, computational domain $256 \times 256 \times 256$). For comparison: Uniform sampling 1.6×10^7 cells.

(2) into the Poisson or Laplace equation leads to a sparse non-symmetric linear equation system $A\phi = b$, which is solved using a GMRES solver [23].

4.2 Performance and Analysis

Figure 5 shows the number of cells, which is equal to the number of unknowns in the equation system, using an adaptive sampling in a $256 \times 256 \times 256$ computational domain during the simulation of a cloud-to-ground lightning. Compared to a uniform sampling, the number of unknowns for solving the Laplace/Poisson equations is reduced by more than 98% at each step of the simulation.

We computed the average relative error R_ϕ of the potential field in cells adjacent to the discharge

	32^3	64^3	128^3
mean R_ϕ	0.04128	0.04004	0.04348
var R_ϕ	0.00139	0.00149	0.00152
$E[R_p]$	0.06725	0.05058	0.06397

Table 1: Relative error R_ϕ of the adaptive sampling compared to an uniform grid. For each grid size, we computed the relative error of the potential field ϕ adjacent to the discharge pattern at the beginning, in the middle, and at the end of the simulation of a downward negative lightning. $E[R_p]$ is the expectation value of the relative errors of the probability distribution R_p .

pattern compared to an uniform sampling. Cells adjacent to the discharge pattern are the locations of possible breakdowns N , and the probability of breakdowns is computed solely based on the potential field of these cells (see equation 1), therefore only the field at these locations is relevant for our simulation. We simulated the stepped leader of a cloud-to-ground lightning and computed the relative error at the end of the simulation. Our results summarized in Table 1 show that all average relative errors are smaller than 5%. Since lightning propagation is a stochastic process, the errors have no noticeable influence on the result. We also list the expectation value $E[R_p]$ of the relative error of the probability distribution R_p . The probabilities are computed using equation (1) with $\eta = 2$.

5 Residual Positive Charge Simulation

After each lightning stroke, residual positive charge (RPC) remains along the path of the lightning. RPC influences the breakdown pattern of successive lightnings because it changes the potential field ϕ . We assume that RPC are particles carrying positive charge. As these particles are moved, for example by air flow, the electric field, and hence subsequent lightning strokes, are influenced by their surroundings.

We predict the movement of the RPC using a particle system [24]. After a lightning stroke is computed, the amount of RPC along its channels is determined, and for each cell that contains RPC, particles are generated. The goal is to determine the position of the RPC at the time of the next breakdown. The particles are advected using a velocity field computed by a simple fluid simulation, and then mapped it back into our adaptive data structure. To place the RPC as accurately as possible, all cells at the location of RPC particles are subdivided to the finest level. Figure 6 illustrates the RPC simulation.

6 Rendering

We adapt the method of Kim et al. [1] and Narasimhan and Nayar [17] to model multiple scattering of light in the presence of bad weather or mist. The typical glow around a point light source captured by a camera can be described with an analytical expression, called the *Atmospheric Point*

Spread Function (APSF). It can be controlled by two intuitive parameters, a scale factor σ that denotes the fraction of flux lost within a unit volume of the atmosphere, and an approximate forward scattering parameter q that captures the weather condition, such as normal air, small aerosols, haze, mist, fog, or rain. The glow of a lightning is made up by the sum of a multitude of point light sources with varying intensities I along the discharge pattern.

Intensities are assigned using a heuristic [1]. The discharge pattern is interpreted as a tree structure, and the line segments connecting the nodes are classified into three different categories: main channel, secondary channels and side channels. For each of these categories an intensity value is manually assigned.

In previous work [1, 17] it was assumed that the distance to all point light sources is approximately the same, and the image of a light source of arbitrary shape was written as a convolution $(I \cdot S) * APSF$, where S represents the shape function that is constant over the extent of the light source. This assumption does not hold in our case, because our simulation takes place in 3D and distances between camera and different parts of the lightning could vary significantly. We therefore split our discharge pattern into several layers depending on the distance to the camera, and compute the APSF for each of them independently. Based on the superposition principle of light these layers are added up resulting in the final image of the lightning.

To combine a lightning with an arbitrary scene, we add point light sources at the lightning position to the scene. The lightning and the scene are rendered independently and are combined using the intensities in the lightning image as alpha values.

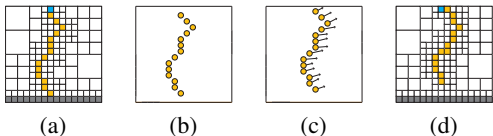


Figure 6: *RPC Simulation: (a) After a lightning stroke RPC remains in the air. (b) For each cell that contains RPC, particles are generated. (c) Advection of particles along air flow. (d) Particles are mapped back onto grid before simulating the next lightning stroke.*

7 Results

We simulated an ascending electric arc between two wires using the RPC simulation. The electric arc moves upwards, because air along the path of an electrical discharge is heated up by the current and can reach temperatures up to 28,000 kelvin [25]. This leads to air movement that influence the RPC and consequently the electric field. An example of this effect is shown in Figure 7.

As initial condition, charges are inserted for modeling the wires. The left and right wire is set to the potential $\phi = 0$ and $\phi = 1$ respectively. All cells belonging to the left wire are considered as places for the initial breakdown, so the discharge pattern could start growing from each of these cells. In our example, as expected, the first discharge takes place where the two wires are closest to each other.

Along the lightning stroke, particles representing the RPC are generated. A simple fluid simulation computes a velocity field which we apply to the RPC. Particles that leave the computational domain are deleted, and we neglect particle-particle interactions in our simulation.

Because the velocity field points predominantly upward and the RPC attracts the growing discharge pattern during each breakdown, the animation of several consecutive breakdowns results in an ascending electric arc.

Figure 8 shows renderings of negative cloud-to-ground lightnings with $\eta = 2$. The background in Figure 7 was created with POV-Ray.

Table 2 shows the performance of our algorithm computing a negative cloud-to-ground lightning, measured on a 2.8 GHz Pentium 4 CPU with 1 GB of RAM.

	64^3	128^3	256^3
# Constr. Cells	4316	17436	69123
Comp. Time [s]	102.7	1895.1	22089.3

Table 2: *Timings for the negative cloud-to-ground lightning ($\eta = 2$, precision 10^{-4}) scenario, in seconds. The number of constrained cells belonging to the lightning pattern and initial charge distribution is an indicator for the complexity of the simulation.*

8 Conclusion

We have presented an adaptive animation technique for electrical discharges. It allows fast physically-based lightning simulations providing high resolution 3D datasets. As the analysis of the relative error shows, the potential field computed based on the adaptive discretization comes close to the original method using a uniform sampling and has no visible effect on the result. However, the computational speed outperforms the uniform grid significantly, making 3D animations feasible. Furthermore, we proposed the simulation of residual positive charge using a particle simulation, which permits us to reproduce the effects of air flow on continuous electrical discharges.

Our adaptive discretization scheme can also be applied to other Laplacian growth phenomenas that are typically simulated using the DBM, such as ice and river formation, fracture, or tree growth. An interesting direction for future work will be to research such applications.

Acknowledgments

The authors want to thank Miguel Otaduy and the anonymous reviewers for their valuable feedback and their help to improve this paper.

References

- [1] T. Kim and M. Lin. Physically-based animation of lightning. In *Proc. of Pacific Graphics '04*, pages 267–275, 2004.
- [2] A. S. Glassner. The digital ceraunoscope: Synthetic thunder and lightning. *Technical Report*, MSR-TR-99-17, April 1999.
- [3] R. D. Hill. Analysis of irregular paths of lightning channels. *Journal of Geophysical Research*, 73:1897–1906, 1968.
- [4] D. M. LeVine and Bruce Gilson. Tortuosity of lightning return stroke channels. *Technical Report*, TM 86104, May 1984.
- [5] T. Reed and B. Wyvill. Visual simulation of lightning. In *Proc. of SIGGRAPH '94*, pages 359–364, New York, NY, USA, 1994. ACM Press.
- [6] P. Kruszewski. A probabilistic technique for the synthetic imagery of lightning. *Computers & Graphics*, 23(2):287–293, 1999.
- [7] B. Sosorbaram, T. Fujimoto, K. Muraoka, and N. Chiba. Visual simulation of lightning taking into account cloud growth. In *Proc. of the Int. Conf. on Computer Graphics '01*, page 89, Washington, DC, USA, 2001. IEEE Computer Society.
- [8] E. R. Mansell, D. R. MacGroman, C. L. Ziegler, and J. M. Straka. Simulated three-dimensional branched lightning in a numerical thunderstorm model. *Geophysical Research*, 107(D9), 2002.
- [9] T. Kim, J. Sewall, A. Sud, and M. C. Lin. A fast fractal growth algorithm. In *Technical Sketch: SIGGRAPH '05*. ACM, Aug 2005.
- [10] A. D. Polyinin. *Handbook of Linear Partial Differential Equations for Engineers and Scientists*. Chapman & Hall/CRC Press, 2002.
- [11] F. Gibou, R. P. Fedkiw, L. Cheng, and M. Kang. A second-order-accurate symmetric discretization of the poisson equation on irregular domains. *J. Comput. Phys.*, 176(1):205–227, 2002.
- [12] C. Min, F. Gibou, and H. D. Ceniceros. A supra-convergent finite difference scheme for the variable coefficient poisson equation on fully adaptive grids. *J. Comput. Phys.*, 2006. to appear.
- [13] H. Johansen and P. Colella. A cartesian grid embedded boundary method for poisson's equation on irregular domains. *J. Comput. Phys.*, 147(1):60–85, 1998.
- [14] W. L. Briggs, V. E. Henson, and S. F. McCormick. *A multigrid tutorial: second edition*. Society for Industrial and Applied Mathematics, Philadelphia, PA, USA, 2000.
- [15] M. Berger and J. Olinger. Adaptive mesh refinement for hyperbolic partial differential equations. *J. Comput. Phys.*, 53:484–512, 1984.
- [16] Y. Dobashi, T. Yamamoto, and T. Nishita. Efficient rendering of lightning taking into account scattering effects due to cloud and atmospheric particles. In *Proc. of Pacific Graphics '01*, page 390, Washington, DC, USA, 2001. IEEE Computer Society.
- [17] S. G. Narasimhan and S. K. Nayar. Shedding light on the weather. In *IEEE CVPR*, 2003.
- [18] L. Niemeyer, L. Pietronero, and H. J. Wismann. Fractal dimension of dielectric breakdown. *Phys. Rev. Lett.*, 52(12):1033–1036, Mar 1984.
- [19] M. B. Hastings. Fractal to nonfractal phase transition in the dielectric breakdown model. *Phys. Rev. Lett.*, 87(17), Oct 2001.
- [20] J. Sañudo, J. B. Gómez, F. Castaño, and A. F. Pacheco. Fractal to nonfractal phase transition in the dielectric breakdown model. *Nonlin. Processes Geophys.*, 2:101–106, 1995.
- [21] M. D. Noskov, V. R. Kukhta, and V. V. Lopatin. Simulation of the electrical discharge development in inhomogeneous insulators. *Journal of Physics D*, 28:1187–1194, 1995.
- [22] P. DuChateau and D. Zachmann. *Applied Partial Differential Equations*. Dover Publications, 2002.
- [23] Y. Saad and M. H. Schultz. Gmres: a generalized minimal residual algorithm for solving non-symmetric linear systems. *SIAM J. Sci. Stat. Comput.*, 7(3):856–869, 1986.
- [24] W. T. Reeves. Particle systems \dot{U} technique for modeling a class of fuzzy objects. *ACM Trans. Graph.*, 2(2):91–108, 1983.
- [25] D. R. Lide. *CRC Handbook of Chemistry and Physics*. CRC Press, 1996.



Figure 7: *Ascending electric arc between two wires.*

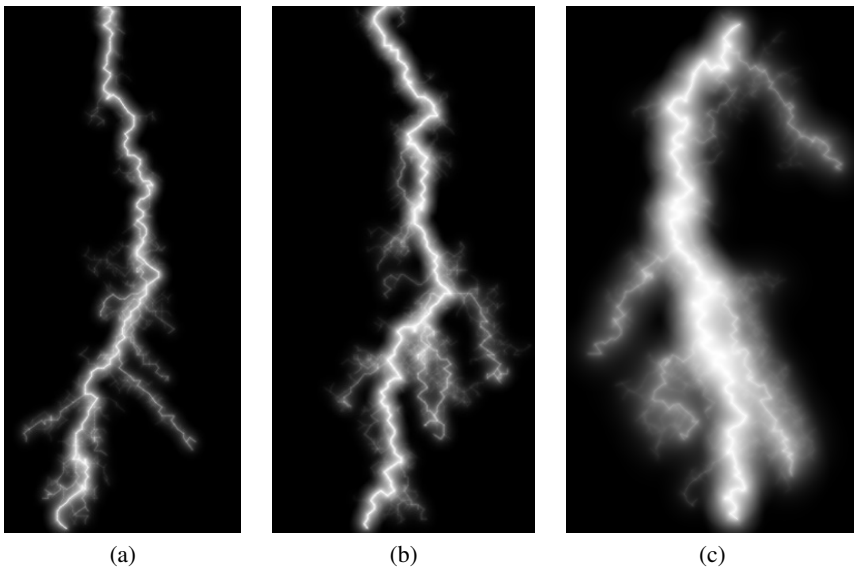


Figure 8: *Downward negative lightnings. (a) and (b) are simulated on a 128^3 , (c) on a 256^3 grid.*